

Characteristics of GaN-based LED fabricated on a GaN-on-silicon platform

To cite this article: Zheng Shi *et al* 2014 *Appl. Phys. Express* **7** 082102

View the [article online](#) for updates and enhancements.

You may also like

- [Optical and structural characterization of GaInN/GaN multiple quantum wells grown on nonpolar a-plane GaN templates by metalorganic vapor phase epitaxy](#)
Shunya Otsuki, Daiki Jinno, Hisayoshi Daicho *et al.*
- [11.2 W/mm power density AlGaIn/GaN high electron-mobility transistors on a GaN substrate](#)
Yansheng Hu, Yuangang Wang, Wei Wang *et al.*
- [Impact of epitaxial strain relaxation on ferromagnetism in a freestanding \$\text{La}_{2/3}\text{Sr}_{1/3}\text{MnO}_3\$ membrane](#)
Ryuji Atsumi, Junichi Shiogai, Takumi Yamazaki *et al.*

Characteristics of GaN-based LED fabricated on a GaN-on-silicon platform

Zheng Shi, Xin Li, Gangyi Zhu, Zhenhai Wang, Peter Grünberg, Hongbo Zhu, and Yongjin Wang*

Grünberg Research Centre, Nanjing University of Posts and Telecommunications, Nanjing 210003, China

E-mail: wangyj@njupt.edu.cn

Received March 27, 2014; accepted June 29, 2014; published online July 14, 2014

In this paper, we describe the fabrication and characterization of a GaN-based light-emitting diode (LED) on a GaN-on-silicon platform. A freestanding membrane structure eliminates the absorption of the emitted light by a silicon substrate and reduces the number of confined optical modes, leading to higher photoluminescence intensity. Compared with an LED with a silicon substrate, the current–voltage characteristics of a freestanding membrane LED demonstrate a lower turn-on voltage and a steeper current–voltage profile. Both anomalous positive capacitance peak and negative capacitance are observed in the capacitance–voltage measurements, which correspond well to the current–voltage characteristics. The measured electroluminescence intensity is significantly increased for a freestanding membrane LED. These experimental results show that our proposed substrate removal technology is promising for the fabrication of a high-performance membrane LED for diverse applications. © 2014 The Japan Society of Applied Physics

GaN-based light-emitting diodes (LEDs) and surface-emitting lasers are regarded as the most important light sources in next-generation solid-state lighting owing to advantages in energy efficiency, long lifetime, high reliability, environmental protection, safety, and diverse applications.^{1–5} The substrate used for GaN growth is a challenging issue for developing GaN-based light emitters. While the costs of GaN-based LEDs grown on sapphire are dropping, silicon is a very common substrate, and the costs are much lower than that of sapphire. With the breakthrough for growing GaN on silicon by the utilization of a buffer layer,^{6,7} it is promising to fabricate GaN-based optical components on a GaN-on-silicon template.^{8–10} In particular, the LED industry will move to take advantage of the lower-cost silicon substrate. It is of considerable interest to investigate GaN-based LEDs grown on silicon substrates. Zou et al. demonstrated high-performance GaN-based LEDs grown on a SiO₂-nanorod-patterned GaN/Si template.¹¹ Furthermore, silicon micromachining is a mature technique for removing the silicon substrate to generate freestanding GaN membrane devices. Wakui et al. reported on a freestanding membrane LED on GaN-on-silicon for micro-electro-mechanical system application.¹²

In this paper, we demonstrate the fabrication and characterization of a GaN-based LED on a GaN-on-silicon platform. A double-side process is used to remove the silicon substrate and fabricate a freestanding membrane LED. In the front-side process, the LED structure is fabricated. The silicon substrate is then removed through the backside process to form a freestanding membrane LED device. The photoluminescence (PL) and angle-resolved reflectance measurements are carried out to characterize the optical performance. Current–voltage (I – V), capacitance–voltage (C – V), and electroluminescence (EL) measurements are then performed for the fabricated LEDs. The experimental results show significant improvements in the electrical and optical performances of the freestanding membrane LED.

A cross-sectional scanning electron microscopy (SEM) image of a GaN-on-silicon wafer structure is shown in Fig. 1(a). The thicknesses of the p-GaN layer, InGaN/GaN multiple quantum wells (MQWs), n-GaN layer, and buffer layers are 120 nm, 125 nm, 2.8 μ m, and 4.29 μ m, respectively. Thick buffer layers are introduced to overcome the physical mismatch between silicon and GaN crystal lattices and the difference in the thermal expansion coefficients of the

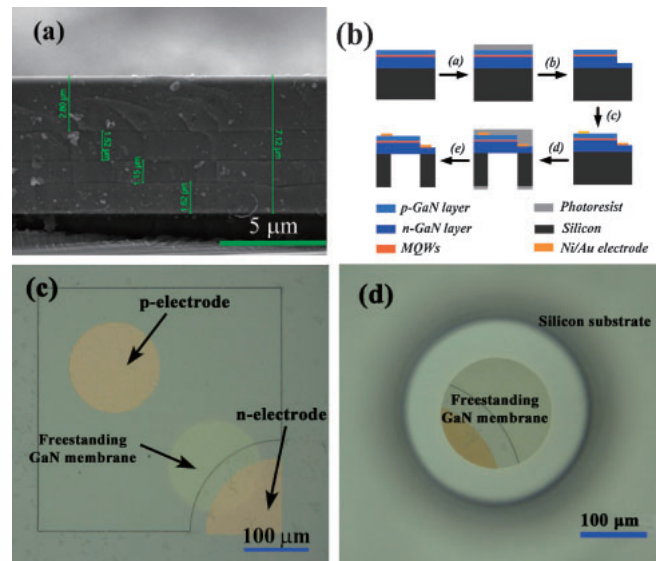


Fig. 1. (a) Cross-sectional SEM image of LED structure; (b) schematic of fabrication of freestanding membrane LED; (c) optical microscopy image of a freestanding LED; (d) optical microscopy image of silicon substrate.

different materials. Figure 1(b) shows a schematic of the fabrication of the freestanding membrane LEDs. An AZ5214 photoresist is first spin-coated onto the p-type GaN layer, and thus the isolation mesa is defined by photolithography (step 1). Then, the epitaxial layers are etched down to the n-GaN layer by reactive ion etching (RIE). Here, Cl₂ and BCl₃ hybrid plasma are used to etch the epitaxial layers with an etching rate of 90 nm/min, and the etching depth is approximately 900 nm (step 2). After removing the residual photoresist, both p- and n-electrode regions are patterned by photolithography and evaporated with 5 nm Ni/15 nm Au layers to serve as the semitransparent metal ohmic contacts (step 3). After lift-off, the devices are annealed in air at 500 °C for 10 min to make the electrodes form ohmic contacts. After protecting the top surface with the AZ5214 photoresist, the silicon substrate is patterned by backside alignment photolithography and removed by deep reactive ion etching (DRIE). DRIE of silicon is conducted with alternating steps of SF₆ etching and C₄F₈/O₂ passivation, and the buffer layer acts as the etching stop layer (step 4). Finally, the freestanding membrane LEDs are generated by removing the residual photoresist (step 5).

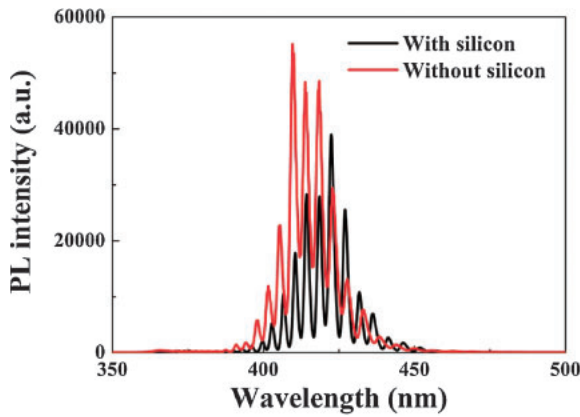


Fig. 2. Measured photoluminescence spectra.

Figure 1(c) shows an optical microscopy image of the fabricated LEDs. The size of the LED is $400 \times 400 \mu\text{m}^2$. The circular p-electrode has a radius of $100 \mu\text{m}$ and the n-electrode has a radius of $150 \mu\text{m}$. The freestanding membrane may not be sufficiently strong to sustain the residual stress when the membrane size is too large. For this consideration, the membrane LED is partially suspended. Figure 1(d) shows the freestanding membrane LED observed from the backside. DRIE is used to create deep penetration and steep-sided holes. In our case, the diameter of the designed circular hole is $200 \mu\text{m}$ and that of the obtained membrane is approximately $142 \mu\text{m}$. Slightly tapered walls are obtained with the tapered angle of 81.5° .

From the optical device point of view, the freestanding membrane improves the light emission. Most of the emitted light is confined within the LED structure owing to the total internal reflection at the GaN surface, and part of the emitted light is absorbed by the silicon substrate. The light emission can be enhanced after removing the silicon substrate. The PL measurement is performed using a microzone confocal Raman spectroscope equipped with a color charge-coupled device camera. A 325 nm He–Cd laser is used as the excitation source. Figure 2 shows the normalized room-temperature PL spectra, which reveal strong emission peaks owing to the excitation of InGaN/GaN MQWs. After removing the silicon substrate, the blue shift of the PL spectra is observed, which is caused by the change in the stress state. Silicon absorption is eliminated, and multiple reflections of the emitted light from the bottom membrane interface enhance the light emission.

Furthermore, there will be a corresponding decrease in the number of confined optical modes as the silicon substrate is removed.^{13,14} Angle-resolved reflectance measurements are performed in the range of 500–850 nm owing to the limitations of the light source and the spectrometer used in our case. Figure 3(a) shows the measured contour plots as functions of wavelength and incident angle for the LED with a silicon substrate. Strong reflectance modulations that are attributed to the optical interferences of the multiple reflections at the different interfaces are clearly observed in the measured contour plots. As the silicon substrate is removed, the number of interference fringes within the wavelength range decreases and the reflectance interference fringes are broadened, as illustrated in Fig. 3(b). Since the number of optical modes inside the GaN layer is membrane-thickness-

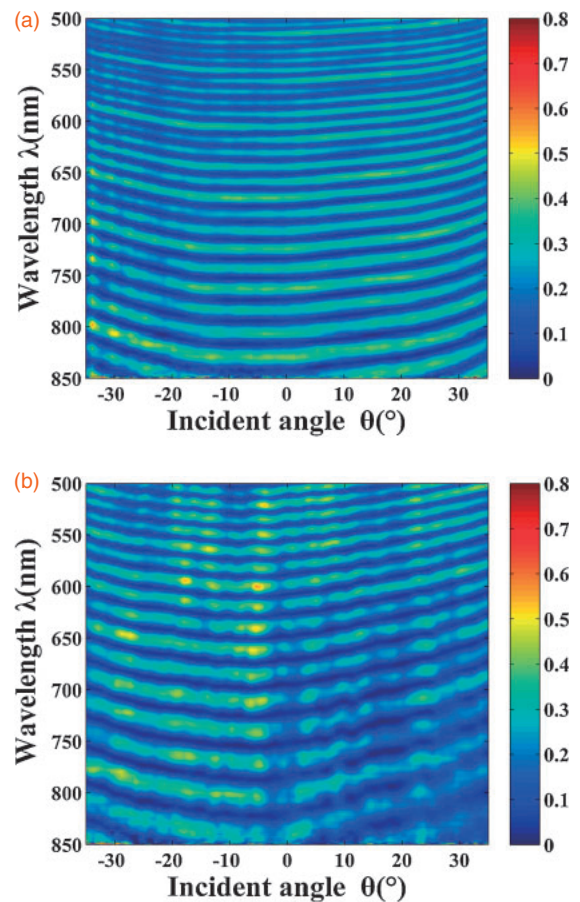


Fig. 3. Angle-resolved microreflectance of fabricated LEDs: (a) LED with silicon substrate; (b) freestanding membrane LED.

dependent and reducing the confined optical modes will lead to an increase in the light emission of the fabricated LED,¹⁵ back wafer etching of the freestanding membrane LED can be further developed as an effective tuning mechanism for the membrane LED. Moreover, the freestanding membrane LED offers potential integration with a cooling system to reduce the thermal resistance for high-power GaN-based LEDs.

I – V and C – V measurements are performed for the fabricated LEDs using an Agilent B1500A semiconductor device parameter analyzer. When the LED is under the forward bias condition, a negative voltage is applied to the n-GaN and a positive voltage is applied to the p-GaN, which decreases the width of the depletion layer.¹⁶ If this forward voltage becomes greater than that of the potential barrier, the LED will be turned on and forward current will start to flow. Figure 4(a) shows the measured I – V characteristics of fabricated LEDs. The p–n junction depth is decreased after the silicon substrate is removed, which leads to the reduction of spreading resistance.¹⁷ Moreover, the release of the built-in residual stress inside epitaxial films may increase the conductivity of the GaN membrane when the silicon substrate is etched through.^{18,19} In our case, the considerable improvement of the I – V characteristics for the freestanding membrane LED may be attributed to the reduction of the spreading resistance and the increase in the conductivity. The turn-on voltage is approximately 1 V lower than that of the LED with the silicon substrate. Figure 4(b) shows the measured capacitance versus forward bias voltage for the fabricated LEDs. The C – V characteristics are measured at a frequency of

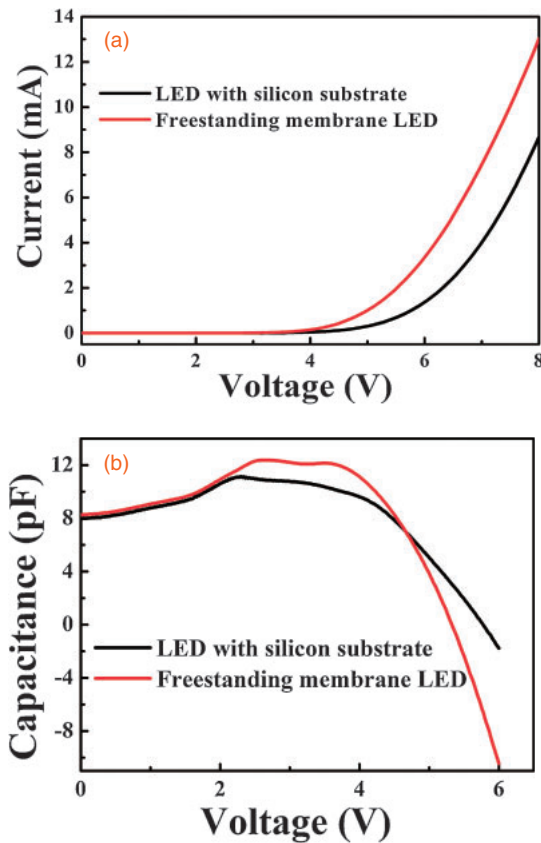


Fig. 4. (a) I - V curves for fabricated LEDs; (b) C - V curves for LED device for fabricated LEDs.

1 MHz and show an increase in capacitance with the increase in the forward voltage, confirming the narrowing of a depletion layer according to the voltage increase. The positive capacitance reaches a peak at approximately the turn-on voltage. It can be seen that the anomalous capacitance peak under forward bias becomes clearer for the freestanding membrane LED.²⁰⁾ In this region, the freestanding membrane LED has a lower series resistance and a higher positive capacitance than the LED with a silicon substrate. Then, the current shown in Fig. 4(a) gradually increases according to the increase in the forward voltage, and the positive capacitance decreases to zero, as illustrated in Fig. 4(b). For the freestanding membrane LED, the steeper I - V profile over an applied voltage of 4.7 V is due to the formation of the low-series-resistance path through the LED, which allows large currents to flow through the LED with a small increase in forward voltage. Correspondingly, the C - V curve enters into the negative region, where the negative capacitance shifts to lower voltage for the freestanding membrane LED and decreases rapidly as the forward voltage increases. The capacitance can be defined as $C = dQ/dV$, where dQ is the differential charge and dV is the differential forward voltage. With continuously increasing forward voltage, the radiative recombination exceeds diffusion. This means that the negative variation of the quantity of injected carriers in the active region results in a negative dQ .^{21,22)} The capacitances of two types of LED finally become negative owing to the positive variation of the forward voltage. The larger slope of the decreasing capacitance curve stands for a more efficient recombination, indicating the higher light emission

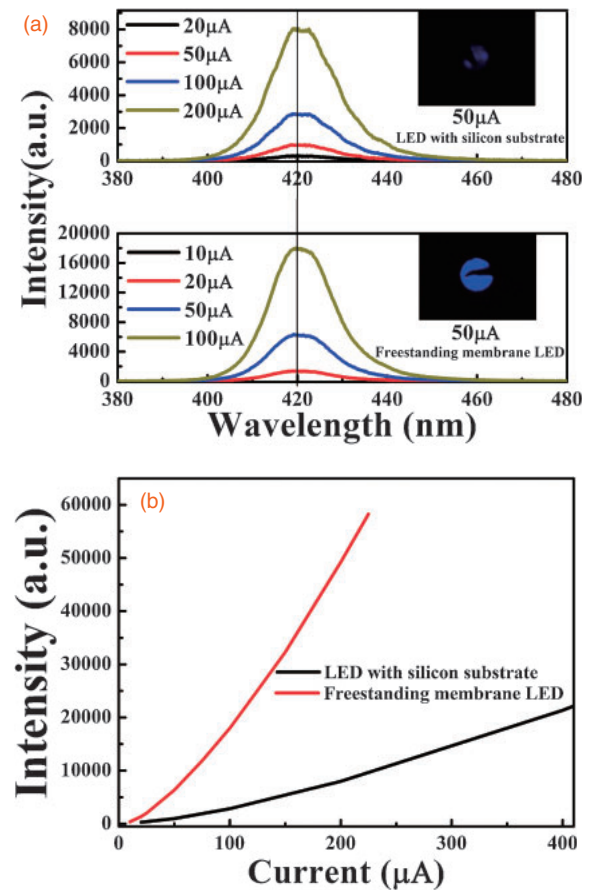


Fig. 5. (a) Room-temperature EL spectra of LED devices under different continuous current injections. Inset: top view of fabricated LEDs under 50 μ A current; (b) peak emission intensity of fabricated LEDs as a function of injection current.

efficiency. With the removal of the silicon substrate, the I - V and C - V characteristics of the membrane LED are improved, and the optical loss is also decreased. In our case, only part of the silicon under the LED is eliminated, whereas the other LED area still sits on the silicon substrate, which indicates that the silicon substrate plays an important role in the optical and electrical performances of fabricated LEDs.

A higher light emission for the freestanding membrane LED is confirmed from the room-temperature EL spectra. Figure 5(a) shows that the GaN-based LED emits incoherent light in a narrow spectral range when a forward bias is applied. Since the membrane LED is partially fabricated, a strong emission peak can be observed at the 420 nm wavelength for both fabricated LEDs. It can be seen in the inset that the freestanding LED has a stronger light emission than the LEDs with the silicon substrate. A large number of confined modes exist in the fabricated LED, and each mode has a different propagation direction. The light absorption of the silicon substrate is eliminated after removing the silicon substrate, and the reflection of the emitted light from the bottom membrane interface also enhances the light extraction from the top surface, leading to a higher light emission for the freestanding membrane LED. Moreover, when the light propagating inside epitaxial films enters the freestanding membrane, the number of confined optical modes is abruptly reduced, and part of the waveguide modes is converted into the direction normal to the surface at the edge of the

freestanding membrane. The light efficiency is also enhanced. Figure 5(b) illustrates the emission intensities of fabricated LEDs as a function of injection current. As the driving current increases, the carrier concentration also increases. The spreading resistance that is due to current crowding will be decreased. Hence, the light output will be continuously increased. The slope for the freestanding membrane LED is steeper and approximately 6 times larger than that of the LED with the silicon substrate. The light emission is significantly improved for the freestanding membrane LED. The measurement is limited by the equipment used, which is saturated when the PL intensity reaches 80,000 a.u.

In conclusion, a substrate removal technology is proposed to fabricate a freestanding membrane LED on a GaN-on-silicon platform. In comparison with the LED with a silicon substrate, the I - V characteristics of the freestanding membrane LED experimentally demonstrate a lower turn-on voltage and a steeper I - V profile, and the C - V results show a stronger anomalous positive capacitance peak and a larger negative capacitance. The freestanding membrane structure eliminates the absorption of the emitted light by the silicon substrate and is helpful for the light emission. The measured electroluminescence intensity is significantly increased for the freestanding membrane LED. The results suggest that the substrate removal technology is promising for the fabrication of a high-performance membrane LED on a GaN-on-silicon platform for diverse applications.

Acknowledgments This work is jointly supported by NSFC (11104147, 61322112) and research project (NY211001, BJ211026, and CXZZ13.0480).

- 1) S. Kamiyama, M. Iwaya, S. Takanami, S. Terao, A. Miyazaki, H. Amano, and I. Akasaki, *Phys. Status Solidi A* **192**, 296 (2002).

- 2) T.-X. Lee, C.-Y. Lin, S.-H. Ma, and C.-C. Sun, *Opt. Express* **13**, 4175 (2005).
- 3) M. R. Krames, O. B. Shchekin, R. Mueller-Mach, G. O. Mueller, L. Zhou, G. Harbers, and M. G. Craford, *J. Disp. Technol.* **3**, 160 (2007).
- 4) J. J. Wierer, A. David, and M. M. Megens, *Nat. Photonics* **3**, 163 (2009).
- 5) C. L. Liao, Y. F. Chang, C. L. Ho, and M. C. Wu, *IEEE Electron Device Lett.* **34**, 611 (2013).
- 6) A. Dadgar, J. Christen, T. Riemann, S. Richter, J. Blasing, A. Diez, A. Krost, A. Alam, and M. Heuken, *Appl. Phys. Lett.* **78**, 2211 (2001).
- 7) T. Egawa, T. Moku, H. Ishikawa, K. Ohtsuka, and T. Jimbo, *Jpn. J. Appl. Phys.* **41**, L663 (2002).
- 8) Y. Wang, F. Hu, Y. Kanamori, H. Sameshima, and K. Hane, *Opt. Express* **18**, 2940 (2010).
- 9) J. Lv, Z. Yang, G. Yan, W. Lin, Y. Cai, B. S. Zhang, and K. J. Chen, *IEEE Electron Device Lett.* **30**, 1045 (2009).
- 10) P. F. Tian, J. J. D. McKendry, Z. Gong, S. I. Zhang, S. Watson, D. D. Zhu, I. M. Watson, E. Gu, A. E. Kelly, C. J. Humphreys, and M. D. Dawson, *J. Appl. Phys.* **115**, 033112 (2014).
- 11) X. Zou, K. M. Wong, X. Zhu, W. C. Chong, J. Ma, and K. M. Lau, *IEEE Electron Device Lett.* **34**, 903 (2013).
- 12) M. Wakui, H. Sameshima, F. R. Hu, and K. Hane, *Microsyst. Technol.* **17**, 109 (2011).
- 13) Y. W. Cheng, K. M. Pan, C. Y. Wang, H. H. Chen, M. Y. Ke, C. P. Chen, M. Y. Hsieh, H. M. Wu, L. H. Peng, and J. J. Huang, *Nanotechnology* **20**, 035202 (2009).
- 14) W. L. Yeh, C. M. Fang, and Y. P. Chiou, *J. Disp. Technol.* **9**, 359 (2013).
- 15) S. Noda and M. Fujita, *Nat. Photonics* **3**, 129 (2009).
- 16) S. K. Jeon, J. G. Lee, E. H. Park, J. Jang, J. G. Lim, S. K. Kim, and J. S. Park, *Appl. Phys. Lett.* **94**, 131106 (2009).
- 17) K. K. Ng, R. J. Bayrums, and S. C. Fang, *IEEE Electron Device Lett.* **6**, 195 (1985).
- 18) B. S. Kang, S. Kim, J. Kim, F. Ren, K. Baik, S. J. Pearton, B. P. Gila, C. R. Abernathy, C.-C. Pan, G.-T. Chen, J.-I. Chyi, V. Chandrasekaran, M. Sheplak, T. Nishida, and S. N. G. Chu, *Appl. Phys. Lett.* **83**, 4845 (2003).
- 19) B. S. Kang, S. Kim, F. Ren, J. W. Johnson, R. J. Therrien, P. Rajagopal, J. C. Roberts, E. L. Piner, K. J. Linthicum, S. N. G. Chu, K. Baik, B. P. Gila, C. R. Abernathy, and S. J. Pearton, *Appl. Phys. Lett.* **85**, 2962 (2004).
- 20) Ş. Altındal and H. Uslu, *J. Appl. Phys.* **109**, 074503 (2011).
- 21) C. Y. Zhu, L. F. Feng, C. D. Wang, H. X. Cong, G. Y. Zhang, Z. J. Yang, and Z. Z. Chen, *Solid-State Electron.* **53**, 324 (2009).
- 22) L. F. Feng, Y. Li, C. Y. Zhu, H. X. Cong, and C. D. Wang, *IEEE J. Quantum Electron.* **46**, 1072 (2010).